



Dedicated to innovation in aerospace

NLR-TP-2016-229 | September 2016

Simulation of unmanned aerial vehicles in the determination of accident locations

CUSTOMER: Netherlands Aerospace Centre



NLR – Netherlands Aerospace Centre

Netherlands Aerospace Centre

NLR is a leading international research centre for aerospace. Bolstered by its multidisciplinary expertise and unrivalled research facilities, NLR provides innovative and integral solutions for the complex challenges in the aerospace sector.

NLR's activities span the full spectrum of Research Development Test & Evaluation (RDT & E). Given NLR's specialist knowledge and facilities, companies turn to NLR for validation, verification, qualification, simulation and evaluation. NLR thereby bridges the gap between research and practical applications, while working for both government and industry at home and abroad.

NLR stands for practical and innovative solutions, technical expertise and a long-term design vision. This allows NLR's cutting edge technology to find its way into successful aerospace programs of OEMs, including Airbus, Embraer and Pilatus. NLR contributes to (military) programs, such as ESA's IXV re-entry vehicle, the F-35, the Apache helicopter, and European programs, including SESAR and Clean Sky 2.

Founded in 1919, and employing some 650 people, NLR achieved a turnover of 73 million euros in 2014, of which three-quarters derived from contract research, and the remaining from government funds.

For more information visit: www.nlr.nl

Simulation of unmanned aerial vehicles in the determination of accident locations



Problem area

As part of the aviation regulations in the Netherlands, third party risk models have been developed and are applied in the determination of risks to the people on ground (third parties) due to aircraft departures and arrivals. In the derivation of these models, accident data are required. Such risk model has yet to be developed for unmanned aerial vehicles (UAVs). As foreseen in the future, accidents with increasing UAV use can pose a growing safety risk for the environment. So the challenge is how to safely manage future increase of UAV use.

Description of work

This study explores the use of flight simulation as an alternative for gathering accident data for UAVs since data about UAV accidents are scarce. Simulation models for unmanned aerial vehicle in both a fixed wing and a multi-rotorcraft

REPORT NUMBER

NLR-TP-2016-229

AUTHOR(S)

Y. Haartsen
R. Aalmoes
Y.S. Cheung

REPORT CLASSIFICATION

UNCLASSIFIED

DATE

September 2016

KNOWLEDGE AREA(S)

Third Party Risk and Policy
Report

DESCRIPTOR(S)

Third party risk
Unmanned aerial vehicles
Accident locations
Simulation

(quadcopter) configuration are adapted. Through modelling and computer simulation of flights by these UAV configurations, insight is collected regarding ground impact locations for various UAV failure situations, including motor failure with full, partially or loss of controllable surfaces, and for various UAV flight conditions.

Results and conclusions

In the present study, the use of flight simulation is proved to be useful in the determination of accident locations of UAVs. With the lack of accident data, flight simulation provides a second-best option to gather this data. Simulation models for unmanned aerial vehicle in a fixed wing and a multi-rotorcraft (quadcopter) configuration are adapted. Because simulation environments (inherently) create the same output for the same input parameters, the input parameters of the simulation require a (limited) variation of initial conditions to create a distribution in the accident locations.

Applicability

The results of this study form a starting point for the further development of a safety risk model for UAV use.

GENERAL NOTE

2016 International conference on unmanned aircraft systems (ICUAS'16), June 7-10, 2016, Key Bridge Marriott Arlington, VA 22209.

NLR

Anthony Fokkerweg 2
1059 CM Amsterdam

p) +31 88 511 3113 f) +31 88 511 3210

e) info@nlr.nl i) www.nlr.nl



Dedicated to innovation in aerospace

NLR-TP-2016-229 | September 2016

Simulation of unmanned aerial vehicles in the determination of accident locations

CUSTOMER: Netherlands Aerospace Centre

AUTHOR(S):

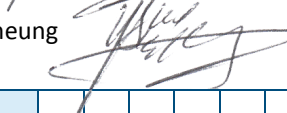
Y. Haartsen
R. Aalmoes
Y.S. Cheung

Delft University of Technology
Netherlands Aerospace Centre
Netherlands Aerospace Centre

2016 International conference on unmanned aircraft systems (ICUAS'16), June 7-10, 2016, Key Bridge Marriott, Arlington, VA 22209.

The contents of this report may be cited on condition that full credit is given to NLR and the authors.

CUSTOMER	Netherlands Aerospace Centre
CONTRACT NUMBER	- - -
OWNER	NLR
DIVISION NLR	Aerospace Operations
DISTRIBUTION	Unlimited
CLASSIFICATION OF TITLE	UNCLASSIFIED

APPROVED BY :														
AUTHOR					REVIEWER					MANAGING DEPARTMENT				
R. Aalmoes 					H. Blom 					P. Eijssen 				
Y.S. Cheung 														
DATE					DATE					DATE	22	09	16	



Simulation of unmanned aerial vehicles in the determination of accident locations

Y. Haartsen, R. Aalmoes, and Y.S. Cheung

Abstract— As part of the aviation regulations in the Netherlands, third party risk models have been developed and are applied in the determination of risks to the people on ground (third parties) due to aircraft departures and arrivals. In the derivation of these models, accident data are required. Such risk model has yet to be developed for unmanned aerial vehicles (UAVs). As foreseen in the future, accidents with increasing UAV use can pose a growing safety risk for the environment. So the challenge is how to safely manage future increase of UAV use.

Because data about UAV accidents are scarce, this study explores the use of flight simulation as an alternative for gathering accident data for UAVs. Simulation models for unmanned aerial vehicle in both a fixed wing and a multi-rotorcraft (quadcopter) configuration are adapted. Through modelling and computer simulation of flights by these UAV configurations, insight is collected regarding ground impact locations for various UAV failure situations, including motor failure with full, partially or loss of controllable surfaces, and for various UAV flight conditions.

I. INTRODUCTION

During the last few years the popularity of unmanned aerial vehicles (UAVs) has increased significantly. UAVs of different sizes are being deployed for military, commercial and private purposes. There are various concerns as to how the UAVs affect the environment, one of which is the safety harm their use poses to property and people. To prevent such harm, currently regulations are very restrictive concerning UAV use. By developing a better understanding of the safety risks that may be posed to the environment by UAV use, it will be possible to safely manage UAV use under far less restrictions. In this perspective one should be aware that for current use of manned aircraft there already exist approaches to safely manage the commercial aviation in the neighbourhood of heavily populated areas. One of the key instruments in doing so is to make use of safety risk models and criteria to assess the risk to the environment and to manage commercial aviation such that the assessed risk level remains below the maximum tolerable level of safety risk.

Third party risk (TPR) concerns the safety (risk) for the people on the ground, who are involuntarily exposed to an aircraft accident. For important economic areas, such as a densely populated area, this impact cannot be neglected. In the Netherlands, numerous studies on TPR around an airport [1] thru [6] have been done, and a TPR model for

conventional aircraft and helicopters has been developed. As one of the few countries in the world, it is now part of Dutch law to determine safety zones around airports in the Netherlands [7].

Although the existing third party safety risk models for commercial aviation are not directly applicable to the use of UAVs, much can be learned from their modelling architecture. The parameters of these existing third party safety risk models are typically based on the collection and statistical analysis of large scale empirical data on aircraft accidents and incidents. As long as UAV use is rather restricted, such data will remain too scarce for a proper parametrisation of safety risk models of UAV use. To overcome these problems, other means of obtaining accident data have to be sought. A possible method is computer simulation of UAV use, under various operational conditions for different UAV configurations and varying sizes. The objective of the work presented in this paper is to explore the use of computer simulation for the development of impact location models for two types of UAVs. The results from the starting point for the further development of a safety risk model for UAV use.

This research focuses on simulation of two types of UAV: rotorcraft and fixed-wing. The rotorcraft considered here is a quadcopter. It is an attractive platform because of its hovering and Vertical Take-Off and Landing (VTOL) capabilities, and good manoeuvrability. The fixed-wing UAV considered here has the appearances of a small aircraft. It is steered through control surfaces similar to that of an aircraft and has comparable aerodynamic characteristics. Since there is no pilot on-board, this allows for light-weight, long-endurance platforms capable of operations that would be too dangerous with a human pilot on-board.

II. LITERATURE ON SAFETY RISK TO POPULATED AREAS

Several previous researches have addressed the determination of the risk to populations due to ground impact of drones. A few often referred are Lum et al [8], Lum and Waggoner [9], Weibel and Hansman [10], Clothier et al [11], Wu and Cothier [12], Dalamagidis et al [13] and Melnyk et al [14].

As suggested in the EU project METROPOLIS, in a foreseen future, the use of Personal Aerial Vehicles (PAVs) and UAVs above a metropolitan or populous area could be considerable. It is therefore necessary to assess the safety impact on the airspace and the environment when these personal or unmanned aerial vehicles were allowed to operate in the air space above populous areas. In the context of METROPOLIS, a rudimentary model [15] has been set up for assessing the risk of PAVs to third parties on ground in the comparison of various ATM-scenarios. In the assessment

Y. Haartsen is student at the Control and Simulation Department, Faculty of Aerospace Engineering, Delft University of Technology, The Netherlands (e-mail: yhaartsen@gmail.com).

R. Aalmoes and Y.S. Cheung are with Aerospace Operations Environment and Policy Support Department, Netherlands Aerospace Centre NLR, Amsterdam, The Netherlands (e-mail: Roalt.Aalmoes@nlr.nl, Yuk.Shan.Cheung@nlr.nl).

it is assumed the model is also applicable for small UAVs. The model's set-up is based on the existing framework of third party risk model [2], which is comprised of three model components: accident probabilities, accident location probabilities, and accident consequences. Adopted in the rudimentary model are parameters derived from the existing risk models for fixed-wing aircraft and helicopters, and literature reviewed.

Specifically introduced in that model for the PAVs and UAVs is the capability of evaluating risk in the cruise or en-route phase of flight. So far, this capability is not required and thus omitted in the third party risk models developed by NLR for large airports [3], regional airports [4] and ground heliports [5]. This is due to the fact that these models are primarily applied in the determination of risk to third parties located due to aircraft departures and arrivals for an airport.

For the cruise or en-route phase of flight, the PAV or UAV follows a certain flight path or aircraft route. Per unit of time and distance along the path, a potential impact area is determined in which the aircraft could impact, See Figure 1. An elliptical shaped impact area is proposed in the model. This area is described by a bivariate normal distribution, where the variance of the length is twice the variance of the width, and the outer limits depend on the glide angle of the vehicle. The elliptical area only applies to fixed wing PAVs or UAVs. For quadcopters a circular area is proposed.

In order to refine the modelling of accident locations in the rudimentary model, research on UAV accidents is necessary. Since, as mentioned earlier, accident data are scarce for UAVs, it is justified to use flight simulation to obtain crash locations. The use of such method has already been explored by Wu and Clothier [12].

III. SIMULATION MODELS

Two most commonly used drone configurations, a rotorcraft and a fixed wing, are considered in the simulation of crashes. Since the dynamics of a rotorcraft are completely different from a fixed wing platform, two different models were needed. The type and size of simulated UAV depend on available data and software. Requirements for the simulation models are that they are accurate, adaptable, time effective and they provide the possibility to simulate multiple UAV types. For the multi-rotorcraft, a model recently developed is

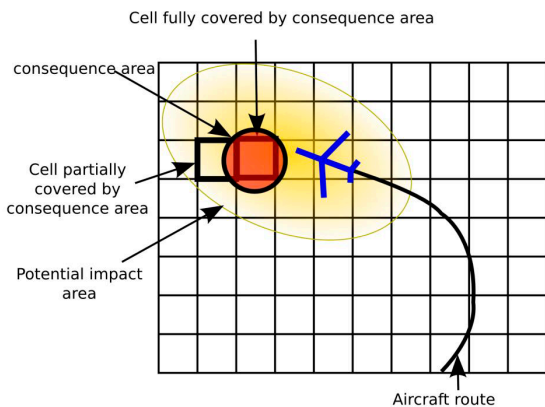


Figure 2. Accident location probability and potential impact area of a single aircraft track.

TABLE 1. AEROSONDE SPECIFICATIONS

Physical specifications	
Wing span	2.8956 [m]
Wing area	0.55 [m ²]
Empty weight	8.5 [kg]
Gross weight	13.5 [kg]
Performance specifications	
Cruise speed	90 [km/h]
Max speed	193 [km/h]
Max altitude	20,000 [ft]

available for use [16]. For the fixed wing model, it has taken some considerable effort to explore a suitable model for use and to adapt it for the research purpose.

A. Fixed wing model

The AeroSim Blockset developed by Unmanned Dynamics can be implemented in Simulink and is free of charge for non-commercial use. The interested reader is referred to the User's Guide for the mathematical model. The Blockset offers adaptable non-linear 6 Degrees Of Freedom complete aircraft models and several demo UAV models such as the Aerosonde and Navion. Besides the aircraft dynamics, it also implements effects from external factors such as wind, gravity, atmosphere and turbulence. For initial simulations the Aerosonde demo is used, which works well in MATLAB 2015b after a few modifications.

The Aerosonde [17] developed by Textron Systems is a small fixed wing UAV with a weight of 13.5kg. It is a single engine configuration designed for long endurance operations. The Aerosonde has been deployed by the army for surveillance missions but also by research facilities for atmospheric measurements. In 1998 the Aerosonde was the first UAV to cross the Atlantic Ocean. Table 1 lists the physical specifications of the Aerosonde as defined in the Simulink model and the performance specifications as defined by [18].

The Simulink model of Aerosonde is comprised of a set of interconnected blocks. During every time step a signal is sent to the blocks, these blocks perform calculations and deliver the output to other blocks. Eventually the state of the aircraft is obtained, and updated for every time step. Altogether, the information acquired at every time steps gives

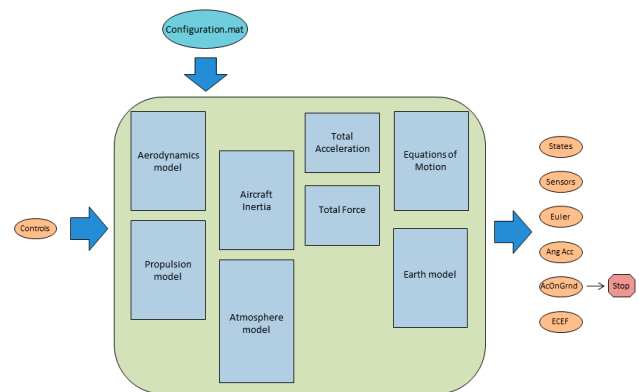


Figure 1. Schematic overview of Aerosonde system architecture with relevant inputs/outputs.

the trajectory of the vehicle.

A schematic overview of the Aerosonde UAV block architecture is shown in Figure 2. Only the relevant inputs and outputs are included. The controls input steers the aircraft. Flaps, mixture and ignition are kept constant while the elevator, aileron, rudder and throttle are controlled to determine the attitude of the aircraft.

There are many possible block configurations to control and aircraft. In the end the system has to meet the mission requirements. In this case, altitude, airspeed and heading are kept constant. An altitude hold loop, yaw damper, auto throttle and wing leveller were added to the model based on the information presented in [19]. After having tested several configurations, only those proved to give the best performance are selected.

In some control blocks saturation limits have been applied in order to prevent unrealistic dynamics. For example, throttle input is set to be between 0 (zero power) and 1 (full power). The saturation limits were determined after analysing the behaviour of the UAV for different control inputs. Subsequently a trim model provided with the block set was used to roughly determine maximum rudder and aileron deflection for a steady turn.

B. Rotorcraft model

The multi-rotorcraft UAV simulation model is a quadcopter model obtained from the Dr. One project [20]. The model, coded in MATLAB, is available for use in the present study. The mathematical formulation is found in [16]. It is adapted from a high order standard helicopter and transformed into a tailless quadcopter, symmetric around one axis. The quadcopter considered in the Dr. One project is a hybrid model. A unique feature of this quadcopter is that it can be equipped with a set of wings, and is thus capable of fixed wing flight. The combination of good manoeuvrability, VTOL and long endurance makes the drone very suitable for medical emergency aid in remote and rural areas. For the simulations in the present study however, the quadcopter is considered as a conventional quadcopter without wings.

The specifications of the quadcopter can be found in Table 2. Since the model is not based on an existing quadcopter, the aerodynamic fuselage data are derived and scaled from a current helicopter.

Due to the high accuracy of the MATLAB model the simulation is slow. One second of simulation time equals approximately 40s of real time on a present-day laptop computer¹. Depending on the initial height and velocity of the quadcopter and the amount of runs simulation could take a few days.

Before a crash can be simulated the quadcopter has to be stable and fly straight or hover. With the model many trim conditions are provided that can be loaded into the main script. It allows for steady flight in six directions with a certain velocity.

A schematic overview of the model can be found in Figure 3. The trim file gives the initial states of the

quadcopter. The variables for the rotation speed of the rotors and the altitude are then overwritten by a MATLAB script. The angular velocity (ω) of each rotor can be defined individually. Since there is no feedback control the quadcopter is highly unstable, in most cases a disturbance leads to loss of altitude and consequently a crash.

IV. SIMULATION SET-UP

As mentioned, the goal of this research is to determine impact location and parameters of UAVs. A collection of impact locations marked a so-called “influence area”. In this context, the influence area is the area affected by a failing unmanned vehicle. It shows the entire area in which an UAV might hit the ground when it fails. The edges of this area can be found by simulating the trajectory of the UAV.

In order to find the impact location, the trajectory of the UAV is simulated when it experiences failure. A crash can have many causes; motor failure, loss of control, loss of communication, mid-air collision, fire and structural failure are a few examples. Many causes are interconnected or arbitrary, and are therefore difficult to simulate. In this study only motor failure will be considered as a direct cause for a crash. As a result, the UAV will continue in a gliding flight or behave as a projectile.

A. Fixed wing aircraft simulation

When the motor of a fixed wing UAV fails and the UAV continues into gliding flight, the resulting impact locations mark the outer boundary of the influence area. In the simulations, the roll angle serves as input is set between -30 and 30 degrees. The timeline of the simulation of the fixed wing UAV is as follows; first the model is stabilized to maintain a given heading, altitude and velocity. After a little less than 60 seconds, the UAV flies steadily and a turn is initiated by giving a step input to the ailerons in order to achieve the desired roll angle. Merely a few seconds later, at 60 seconds, the throttle is then set to 0%. The simulation is repeated for different roll angles.

For some UAVs, to increase safety, the control system and propulsion system are connected to different power sources. Whenever the propulsion system fails the control system might still work, albeit partially. From this, three possible scenarios can be devised.

First, the aircraft is fully controlled, thus the elevator, ailerons and rudder are still capable of stabilizing the UAV. The elevator will maintain the trim altitude at all costs. At some point the deflection of the elevator is too extreme and the simulation is terminated due to calculation errors. Therefore, a saturation limit is applied to the elevator. The

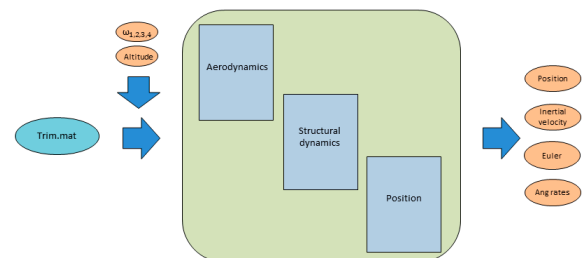


Figure 3. Schematic overview of quadcopter system with inputs/outputs.

¹ Provided with a i5 processor and a Windows 64 bit operating system

chosen value for the saturation limit will possibly influence the maximum distance to the impact location. Meanwhile the ailerons and rudder collaborate on maintaining the desired roll angle.

The second option is full loss of control. In this case, every control surface freezes when the motor fails. If the UAV has just initiated a turn it will generally continue into a spiralling descent. Also the unbalanced roll moment caused by the single engine will drive the UAV towards the left.

The third and last option that will be considered is partial loss of control, in this case lateral control. The ailerons will still function properly and the UAV will descend with a constant roll angle. Since the roll angle is maintained constant throughout the simulations, the resulting trajectory pattern should be symmetrical around the direction of flight. This procedure is similar to that of Wu and Clothier [12] but they simulated a Cessna 172 and did not have to compensate for the unbalanced roll moment produced by the single engine.

B. Rotorcraft simulation

When the quadcopter experiences motor failure the impact location is difficult to predict. It is due to the fact that the quadcopters does not have gliding capabilities. Furthermore, it depends on which rotor fails, the altitude, and to what extent the quadcopter descends in certain direction. Instead of a contour of the influence area, the outcome of the simulation is more likely a collection of scattered points.

The timeline of the simulation is different from that of the fixed wing model since the quadcopter is already in trimmed state when the simulation starts running. Upon starting the simulation the angular velocity of the propellers is immediately overwritten. Since the model lacks a controller the quadcopter will not be stabilized and a disturbance is sufficient for a crash. The rotation will be set at 100%, 75%, 50% and 0% of the initial speed. Initially 25% was also a setting but it proved to be the most insignificant setting. By disregarding the 25% setting, the required number of runs decreased drastically from 624 to 255. Given that the setting where every rotor is at 100% is ignored as well.

Each run basically represents a unique combination of angular velocities. For example run #1: R1 at 100%, R2 at 50%, R3 at 50% and R4 at 0%; run #2: R1 at 0%, R2 at 0%, R3 at 75% and R4 at 100%. Data are compiled for each run for different initial altitude and velocity.

V. RESULTS

A. Fixed wing simulation results

The fixed wing model has been simulated with varying height, velocity, and control scenario. It turned out that even

TABLE 2. QUADCOPTER SPECIFICATIONS

Total weight	1.08 [kg]
Fuselage length	0.6 [m]
Fuselage width	0.4 [m]
Fuselage height	0.1 [m]
Rotor radius	0.127 [m]
Nominal rotor angular velocity	6000 [RPM]

at small roll angles the UAV deviates from the y-axis a lot. Therefore, to obtain an explicit boundary, more roll angles have been added to the original set. These 30 extra roll angles vary between -3 and 3 degrees, adding up to a total amount of 60 inputs for the roll angle. Consequently, in the results, the concentration of impact locations is higher between the -3 and 3 roll angle than for other angles. For the interpretation of the plots it is important to keep in mind that the vehicle initially flies in the direction of the positive x-axis.

1) Control scenarios

For the fixed wing UAV there are three possible situations for control; full control, lateral control only, and no control. In the first situation the current attitude of the vehicle is fed back to the control surfaces. Elevators, ailerons and rudder are still trying to stabilize the aircraft and maintain a certain airspeed and altitude. In the second situation the ailerons still function properly and continue an initiated turn with a given roll angle. Meanwhile the elevator keeps its

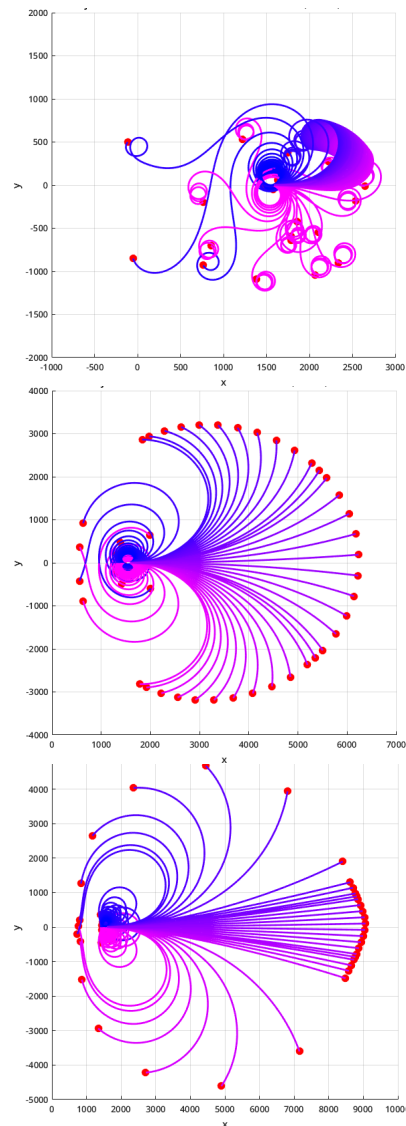
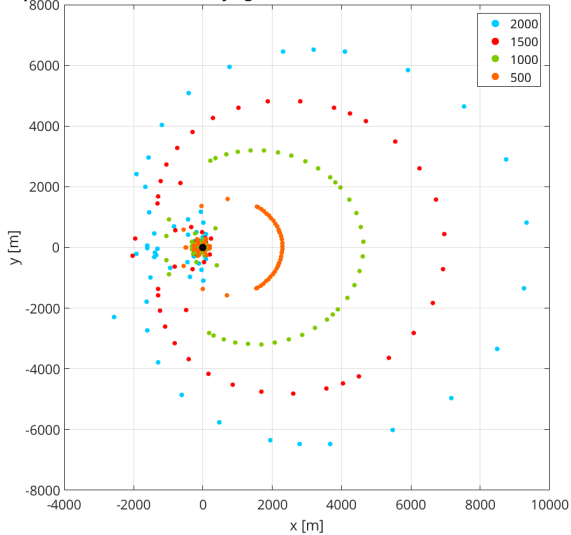


Figure 4. Comparison of trajectories of Aerosonde flying at 1000 feet with 25 m/s for different scenarios of control: no feedback control (upper), lateral only (middle) and full control (lower). The varying track colours indicate different initial roll angles of the aircraft. The x- and y-axes are in metres.

angle as it was just before motor failure. The last situation switches off all control surfaces and holds the current deflections.

Figure 4 shows the results of three simulations for the three different scenarios with equal velocity (25 m/s) and altitude (1000ft). There is a significant difference between the trajectories and the scatter of impact locations. For the scenario where there is no control, the locations are concentrated within a small area. The trajectories show that the UAV goes into a spiral descent close to the location of failure. The asymmetrical pattern is caused by the rolling moment induced by the single engine. On the contrary, the full control scenario leads to a large dispersion, particularly in direction of flight. At low roll angles the UAV does not deviate much from the y-axis, as is the case for the lateral control scenario.

Impact locations Aerosonde flying at variable initial altitude, 25m/s, lateral control



Impact locations Aerosonde flying at variable initial altitude, 25m/s, full control

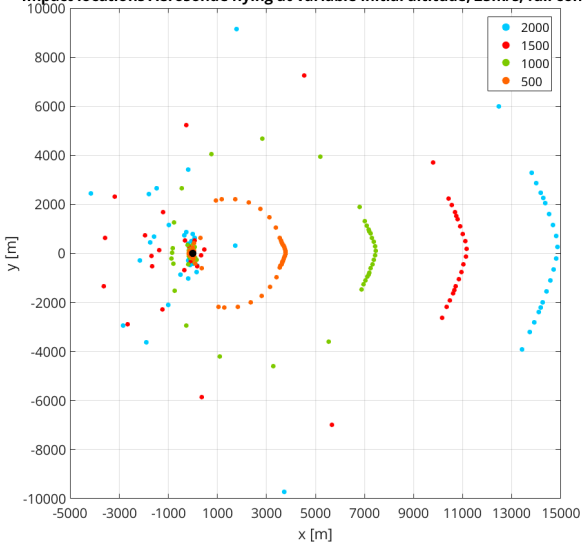


Figure 5. Comparison of impact locations of Aerosonde based on variable initial altitude for lateral (upper) and full (lower) control scenarios. Presented are 500, 1000, 1500, and 2000 ft.

2) Altitude

Since lateral control gives a symmetrical trajectory pattern, for the sake of clarity, only the full control and lateral control scenarios will be used in the comparison for varying altitude (Figure 5). The altitude is increased by 500ft each time. An important observation is that, for high altitudes, the UAV might also end up behind the location where failure began. Also, it is noteworthy that the scatter of the impact locations for lateral control has a somewhat elliptical shape. Along the boundary of this ellipse the impact locations are more evenly distributed for high initial altitudes than for low altitudes. This is logical, since for high altitude the UAV is capable of turning for a longer period of time before reaching the ground.

For the full control scenario the UAV maintains the desired altitude until the elevator deflection is at the saturation limit. Thus for high altitudes the UAV maintains both the roll angle and altitude for some time. This leads to a high concentration of impact locations either close to the failure point or far along the x-axis.

3) Velocity

Velocity was set at 15, 25, 30, 35 and 45 m/s. Figure 6 shows the resulting impact locations when these velocities are applied in the simulation model with lateral control. As can be seen, at higher velocities the impact location of the UAV is much closer to the failure location than at low velocities. This seems counter intuitive. It is conjectured that the disproportional relationship between initial velocity and impact location was caused by the aircraft attitude during straight flight.

B. Rotorcraft simulation results

For the quadcopter model the velocity, direction of flight, altitude, and speed of rotation of the engines have been varied. The data sets consist of 255 runs compiled for each altitude. Every run represents a unique combination of angular velocities. The data is plotted such that north is in the direction of the positive y-axis.

Impact locations Aerosonde at variable initial velocity, 1000ft, lateral control

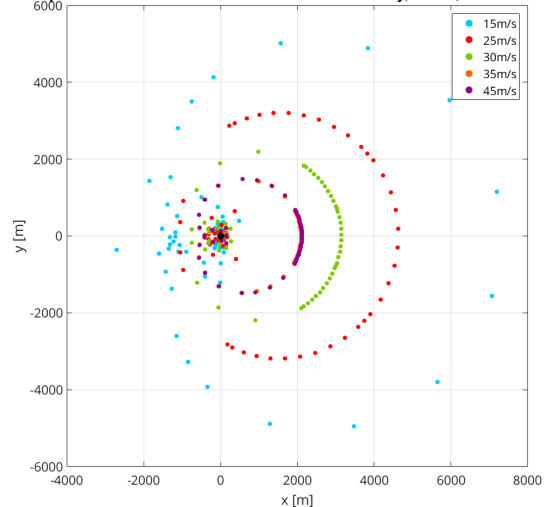


Figure 6. Comparison of impact locations of Aerosonde for various initial velocities at altitude 1000 ft. Presented are 15, 25, 30, 35 and 45m/s.

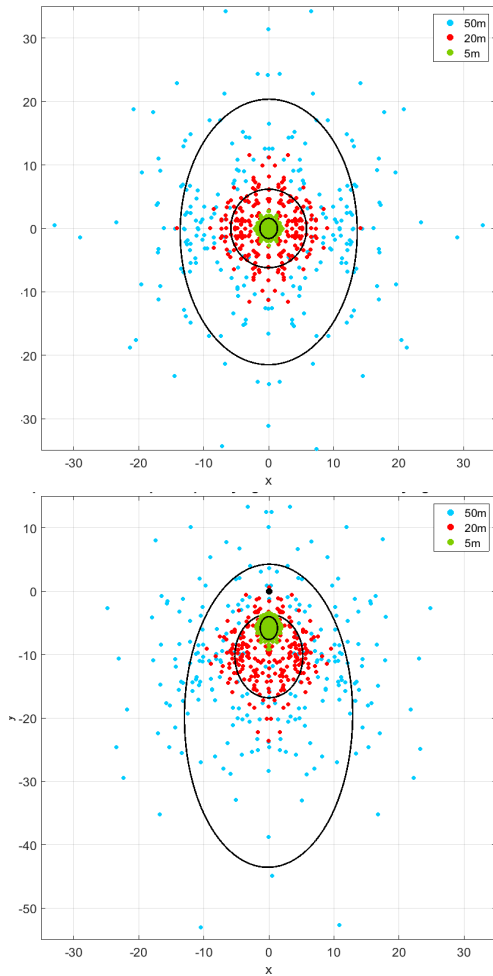


Figure 8. Comparison of impact locations for hovering (upper) and for flying speed 5m/s (lower). Presented altitudes are 5, 20 and 50 metres. The x- and y-axes are in metres.

To get a better impression of the impact location data plot a fit can be applied to the scattered data. By visual inspection a conic shape can be recognized in the data sets. The elliptical fitting method proposed by Fitzgibbon et al [21] is applied here.

1) Altitude

The impact location data for low altitudes is somewhat concentrated and their results are comparable. For high altitudes, however, the data shows a wide spread and the elliptical fit of data with initial altitude of 300 metres can hardly be compared to that of 150 metres or 50 metres. The same holds for 150 metres. Here, only the focus is put on the results for initial altitudes of 50, 20 and 5 metres.

Figure 7 shows the impact locations and the accompanied elliptical fit of a quadcopter hovering at different altitudes. Each point corresponds to a unique combination of angular velocities for each rotor. The shape of the fits deserves some attention. Although the quadcopter is initially hovering above the origin, the impact locations are not distributed in a circular pattern. Instead of this, the spread in y-direction is wider than in x-direction. As shown, the difference increases with altitude.

An explanation for the shape can be based on the physical shape of the quadcopter. The distance between rotor R1 and R4 is one-and-a-half times as much as between R1 and R2. Thus when the quadcopter fails and starts rotating, the behaviour will be different along both axes.

The same simulation has been performed with the quadcopter flying with a velocity of 5 m/s in southern direction (presented as flying into negative direction of y-axis). The results can be found in Figure 7. Note that the black dot indicates the location where the quadcopter fails. The centres of the fits have been shifted in the direction of flight and the fits have a clear elliptical shape. Even though the concentration of impact location is higher within the northern section of the ellipse, the fit for an altitude of 50 metres has an elongated shape. This is due to a single impact location far to the south at (-90.13,-0.79). By and large, the fit can be influenced substantially by an outlier.

2) Velocity

Again the comparison is limited to altitudes of 50, 20 and 5 metres here. Since these three situations are taken into comparison there is a lot of data available. For the sake of clarity, only the elliptical fits are presented in Figure 8. The ellipses are plotted for 5 m/s, 2 m/s and hover. As the velocity of the quadcopter increases, the aspect ratio of the ellipse increases as well.

VI. RESULT ANALYSIS

A. Fixed wing

1) Effects of control scenario on distribution of impact locations

As shown in Figure 4 the trajectories of the Aerosonde under different conditions for feedback control are compared. The Aerosonde deals with the unbalanced roll moment. The case where there is no feedback control shows the consequences of this problem; a chaotic set of trajectories often ending in a spiral descent. Although it is not possible to directly relate the impact location to the initial location, roll angle or

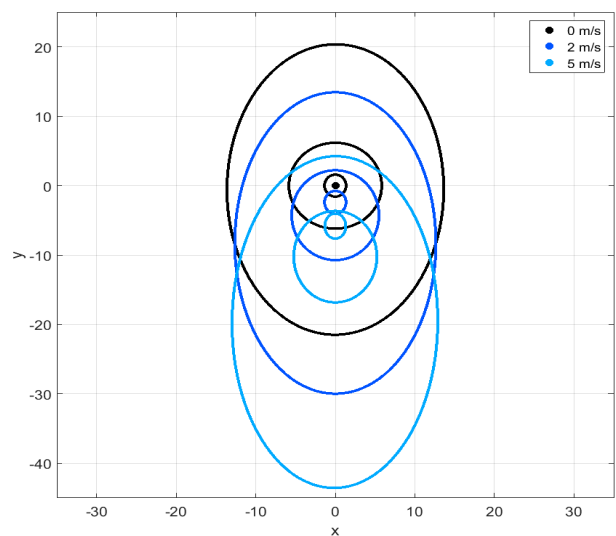


Figure 7. Comparison of elliptical fits based on varying initial velocity and initial altitude. Presented are 0, 2 and 5 m/s. The x- and y-axes are in metres.

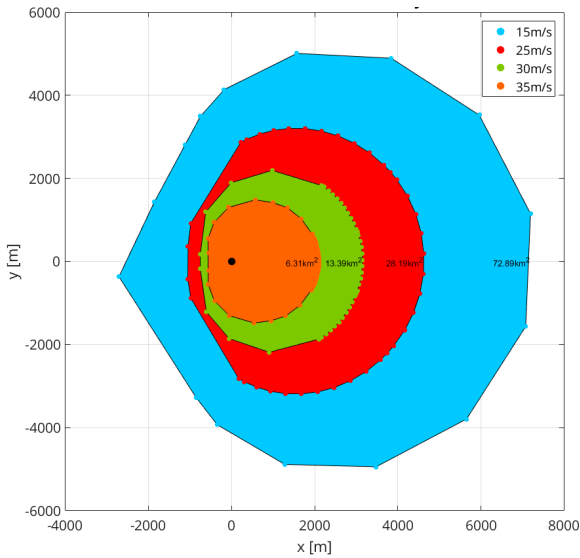


Figure 10. Influence areas defined by impact locations of Aerosonde flying at varying velocities at 1000ft with functional lateral controls. Presented are 15, 25, 30 and 35 m/s.

velocity of the UAV, a positive conclusion can be drawn when it comes to the spread of the impact locations.

First, for most trajectories the vehicle quickly falls into a spiralling descent and therefore crashes close to the location of failure. Thus the impact locations are highly unpredictable and the influence area is definitely smaller as compared to the other scenarios.

Secondly, there is the situation where the attitude of the UAV is fed back to the elevator, rudder and ailerons. Full control leads to a large influence area but the trajectories show a pattern such that it is possible to predict the impact location of the UAV at intermediate roll angles. An important advantage is the removal of the unbalanced roll moment.

Finally, scenario with lateral control lies in between the two latter scenarios. Prediction of the impact location is possible based upon the trajectories of the vehicle, which have a symmetrical shape. Furthermore the influence area is of a significant size but smaller than that of the scenario with full control.

2) *Effects of initial altitude of fixed wing UAV on distribution of impact locations*

To determine the effect of initial altitude on impact location the influence area was determined. Figure 9 shows the influence area, where the impact locations mark the outer boundary. For a flight with a roll angle of 0 degree there seems to be a linear relation between initial altitude and distance to impact location.

3) *Effects of initial velocity fixed wing UAV on distribution of impact locations*

The initial velocities were set at 15, 25, 30, 35 and 45 m/s but since the resulting impact locations of 45 and 35 m/s are almost exactly the same, the data from 45 m/s will be disregarded. This simulation was only carried out for the scenario where there is lateral control. Figure 10 shows the influence area for each initial velocity.

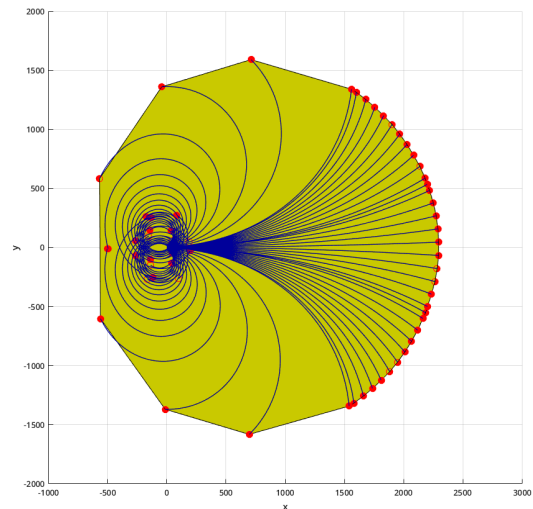


Figure 11. Impact footprint of Aerosonde flying at 500ft initial altitude. The x- and y-axes are in metres.

The initial velocity and maximum distance between impact location and origin are roughly disproportional. Thus if the UAV has a high initial velocity its impact location is closer to the origin than with low initial velocity. This seems contradictory. A further analysis with the use of an animation of the vehicles' attitude during the trajectory reveals the cause. The elevator stabilises the UAV to allow it to fly at the designated velocity and altitude. To maintain the altitude at low velocity a high pitch angle is required to produce sufficient lift. When the motor fails the UAV dips forward due to sudden loss of forward force. This motion is more extreme with a high initial velocity than with low initial velocity; the nose points downward and the vehicle descends very rapidly. With low initial velocity, the attitude of the UAV is such that it pitches slightly upwards, continuing in a gliding descent. Hence it covers a larger distance.

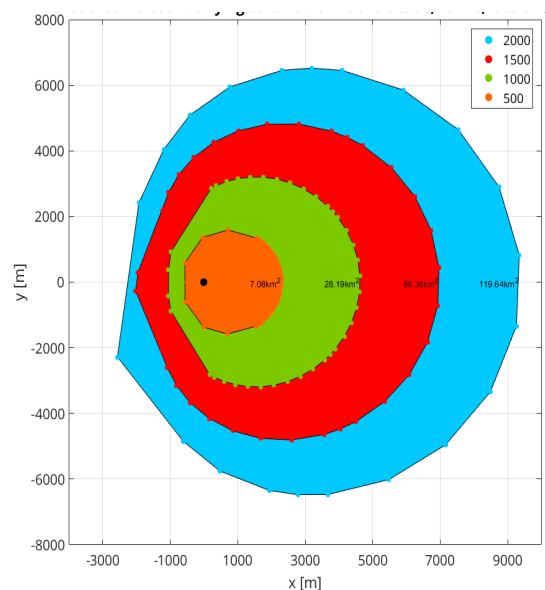


Figure 9. Influence areas defined by impact locations of Aerosonde flying at varying altitudes at 25 m/s with functional lateral control. Presented are 500, 1000, 1500 and 2000 ft.

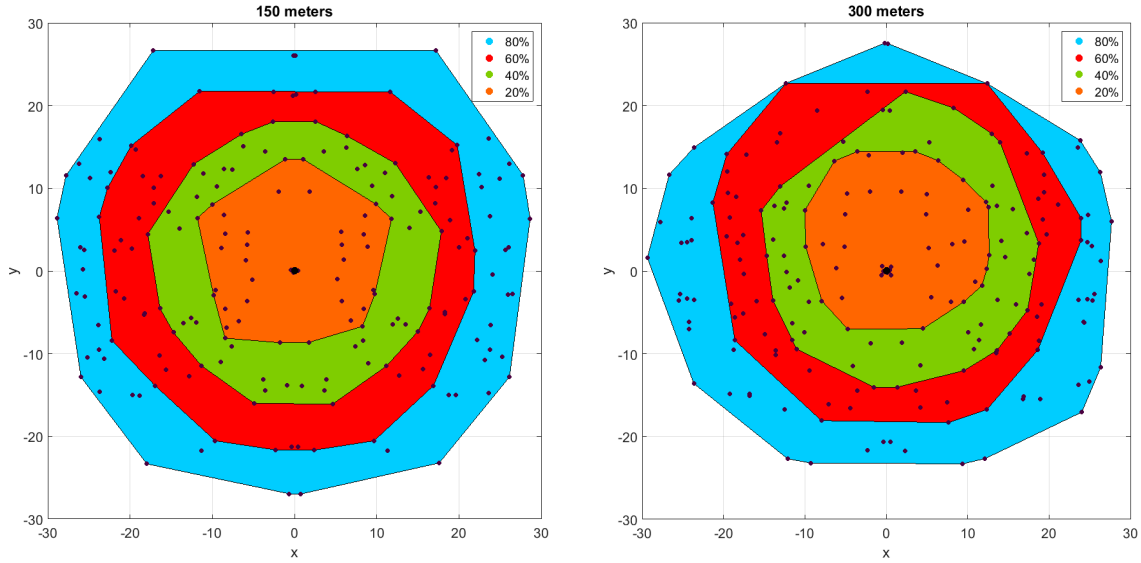


Figure 13. Impact location distribution contours of Aerosonde for two initial altitudes: 150m (left) and 300 m (right). The x-and y-axes are in metres.

4) Comparison with influence area from literature

The impact footprint obtained by Wu and Clothier [12] comes closest to the method used in this project. The authors simulated a Cessna 172 at different initial altitudes, including 500ft. Eventually they come up with a dual ellipse shaped footprint. The shape of their plot is comparable to that of the area depicted in Figure 11, which is the result of a failing Aerosonde flying at 500ft initial altitude. One major difference is the dimension. The area from this project is wider than that of [12] and shifted towards the positive x-direction. Also, according to [12] the UAV does not descend in a spiral trajectory at high roll angles; its trajectory consists of a turn and straight gliding part. Therefore, in the literature, there is also a large part of the influence area behind the failure point. Since both plots are from different aircraft the dimension of the footprint cannot be compared.

B. Rotorcraft

1) Impact location distribution contours

Figure 12 shows the impact location distribution contours for a UAV hovering at an altitude of 300 metres and 150 metres. The two figures below show that 80% of all impact locations occur within an area of 60x60 square metres. For high initial altitude the altitude does not seem to affect the distribution. This is a conspicuous conclusion since it suggests that the impact location lies within a certain region regardless of its initial altitude. The same holds for a quadcopter flying at 5 m/s southbound at 300 and 150 metres, where 80% of the impact locations are also confined within a region of 60x60 square metres.

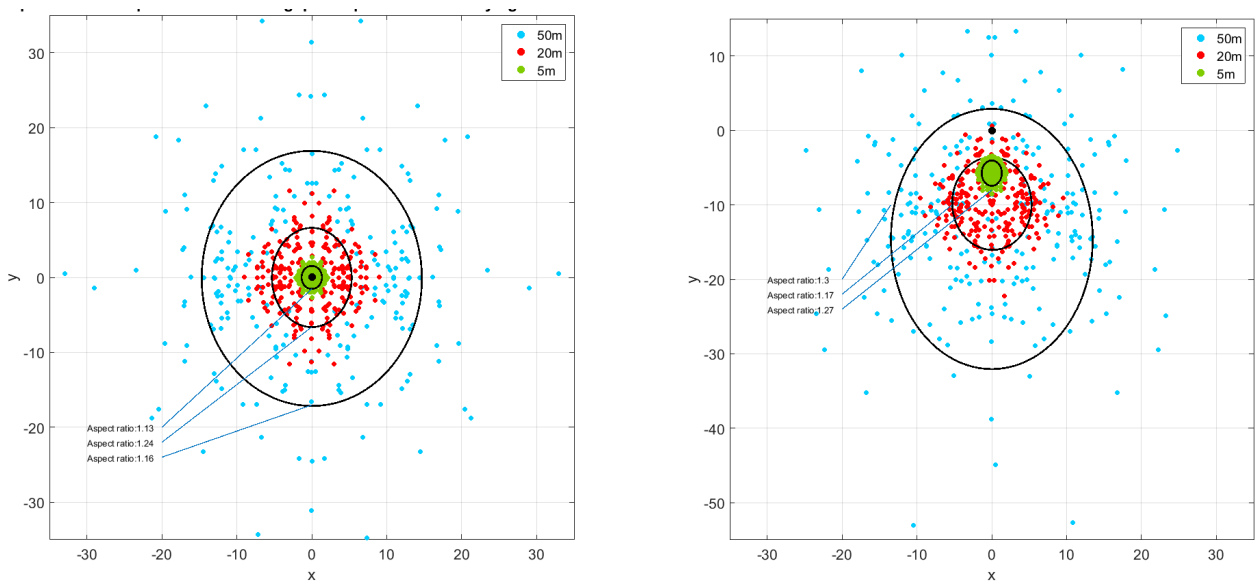


Figure 12. Aspect ratio of elliptical fit based on varying altitudes for two initial velocities of quadcopter: hover (left) and 5m/s (right). Presented are 5, 20 and 50 metres. The x- and y-axes are in metres.

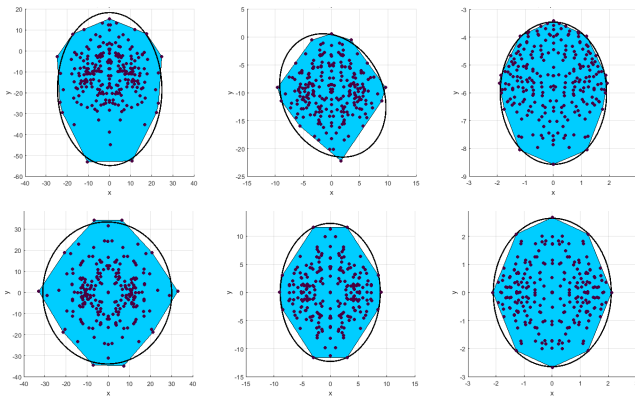


Figure 14. Aspect ratio of potential impact of flying (upper graphs) and hovering (lower graphs) quadcopter based on 99% of the total dataset for varying altitudes. The initial altitude of the quadcopter is from left to right: 50m, 20m, and 5m. See Table 3 for the calculated aspect ratios.

2) Effects of initial altitude of quadcopter on distribution of impact locations

Figure 13 shows the scattered impact locations for different altitudes and the elliptical fit. The aspect ratios for each ellipse are depicted in the bottom left corner. The ellipses for altitudes 150 and 300 metres are not included in the figure. The aspect ratios of the ellipses of a hovering quadcopter are 1.42 for an initial altitude of 150 metres and 1.58 for an initial altitude of 300 metres. For a quadcopter flying at 5 m/s the aspect ratios are 1.66 for an initial altitude of 250 metres and 1.68 for an initial altitude of 300 metres. A conclusion that can be drawn from the aspect ratios at different height is that higher aspect ratios occur at high initial altitude.

3) Comparison with literature

Only one source estimated the distribution of impact locations for a quadcopter. Aalmoes et al [15] suggested an ellipse as potential impact area for a flying quadcopter where the major axis is twice the size of the minor axis. The impact location of 99% of all accidents is within this area. For a hovering quadcopter on the other hand, the potential impact area is circular.

This potential impact area can be reproduced with the results obtained from the project. First a contour has to be determined for 99% of the data. Then an ellipse has to be fitted through the boundary of this contour. For the flying quadcopter the ratio major axis over minor axis is suggested to be 2. A perfect circle would have a ratio of 1.

The results of the current project show an elliptical fit for a flying quadcopter in Figure 14. In Table 3, the corresponding aspect ratios can be found. A ratio of 1 would represent a perfect circle. For the low initial altitude the quadcopter has a more circular shape. The fits for both the

TABLE 3. ASPECT RATIO OF FLYING AND HOVERING QUADCOPTER

Aspect ratio	Initial altitude		
	50 meter	20 meter	5 meter
Flying 5 m/s	1.48	1.28	1.35
Hovering	1.00	1.30	1.26

flying and the hovering quadcopter have an elliptical shape with an aspect ratio between 1.1 and 1.48.

In [12] the centroid of the ellipse coincides with the location where the UAV fails. In Figure 14 it can be found that the centroid of the ellipse lies only on the failure location for the hovering quadcopter. For a flying quadcopter the centroid of the ellipse lies further along the direction of flight.

VII. CONCLUSION

In the present study, the use of flight simulation is proved to be useful in the determination of accident locations of UAVs. With the lack of accident data, flight simulation provides a second-best option to gather this data. Simulation models for unmanned aerial vehicle in a fixed wing and a multi-rotorcraft (quadcopter) configuration are adapted. Because simulation environments (inherently) create the same output for the same input parameters, the input parameters of the simulation require a (limited) variation of initial conditions to create a distribution in the accident locations.

The results of the simulated accident locations show elliptical shaped impact areas; the shape depends on the altitude and initial velocity. These simulations correspond with earlier research, and provide a baseline for future research. These results will also help to improve the current third party risk models for UAVs. Other simulation models of the same kind of UAVs (rotorcraft or fixed-wing) can help to further validate the work done in this study, as well as accident data for UAVs when it becomes available in the future.

ACKNOWLEDGEMENT

The authors would like to thank Henk Blom (affiliated with NLR and Delft University of Technology) for his critical review of this paper and advice on the topic of aircraft safety in general.

REFERENCES

- [1] B. Ale and M. Piers, "The assessment and management of third party risk around a major airport," *Journal of Hazardous Materials* vol. 71, no. 1-3, pp. 1-16, 2000.
- [2] M.A. Piers et al, "The development of a method for the analysis of societal and individual risk due to aircraft accidents in the vicinity of airports," NLR CR 93372 L, National Aerospace Laboratory – NLR Amsterdam, 1993.
- [3] A.J. Pikaar, C.J.M. de Jong and J. Weijts, "An enhanced method for the calculation of third party risk around large airports, with application to Schiphol," NLR-CR-2000-147, National Aerospace Laboratory – NLR, Amsterdam, 2000.
- [4] R.W.A. Vercammen et al, "Re-assessment of the model for analysis of third party risk around regional airports," NLR-CR-2002-178, National Aerospace Laboratory – NLR, Amsterdam, 2002.
- [5] Y.S. Cheung, L. de Haij, J.W. Smeltink and J.M.G.F. Stevens, "A model to calculate third party risk due to civil helicopter traffic at heliports, With the focus on inland heliports in the Netherlands," NLR-CR-2007-003, National Aerospace Laboratory – NLR, Amsterdam, 2008.
- [6] J. Weijts, R. Vercammen, Y. Vijver and J. Smeltink, "Voorschrift en procedure voor de berekening van Externe Veiligheid rond luchthavens," (Report in Dutch: Calculation rules and procedure for third party risk around airports), NLR-CR-2004-083, National Aerospace Laboratory – NLR, Amsterdam, 2004.

- [7] Y.S. Cheung, L. de Haij, and R. de Jong, "Development of NLR third party risk model and its application in policy and decision-making for the airports in the Netherlands," NLR-TP-2013-550, National Aerospace Laboratory – NLR, Amsterdam, 2013.
- [8] C.W. Lum, K. Gauksheim, C. Deseure, J. Vagners and T. McGeer, "Assessing and estimating risk of operating unmanned aerial systems in populated areas," Washington.
- [9] C.W. Lum and B. Waggoner, "A risk based paradigm and model for unmanned aerial systems in the National Airspace," AIAA 2011-1424, Infotech@ Aerospace 2011, 29-31 March 2011, St. Louis, Missouri, 2011.
- [10] R.E. Weibel and R.J. Hansman, Jr., "Safety considerations for operation of different classes of UAVs in the NAS," in AIAA-2004-6421, AIAA's 4th Aviation Technology, Integration and Operations (ATIO) Forum, 20-22 September 2004, Chicago, Illinois, 2004.
- [11] R. Clothier, R. Walker, N. Fulton, D. Campell, "A casualty risk analysis for unmanned aerial system (UAS) operations over inhabited areas," AIAC12 – Twelfth Australian International Aerospace Congress, 2nd Australasian Unmanned Air Vehicles Conference, 19-22 March 2007.
- [12] P.P. Wu and R. A. Clothier, "The development of ground impact models for the analysis of the risks associated with unmanned aircraft operations over inhibited areas," in *Proceedings of the 11th probabilistic safety assessment and management conference (PSAM11) and the annual european safety and reliability conference (ESREL 2012)*, Helsinki, 2012.
- [13] K. Dalamagkidis, K.P. Valavanis and L.A. Piegel, "Evaluating the risk of unmanned aircraft ground impacts," in *16th Mediterranean Conference on Control and Automation*, Ajaccio, 2008.
- [14] R. Melnyk, D. Schrage, V. Volovoi and H. Jimenez, "A third-party risk model for unmanned aircraft system operations," *Reliability Engineering and System Safety*, vol. 124, pp. 105-116, 2014.
- [15] R. Aalmoes, Y.S. Cheung, E. Sunil, J. M. Hoekstra and F. Bussing, "A conceptual third party risk model for personal and unmanned aerial vehicles," 2015 International Conference on Unmanned Aircraft Systems (ICUAS'15), 9-12 June 2015, Denver.
- [16] S. Taamallah, "Small-scale helicopter automatic autorotation, modeling, guidance and control," PhD thesis, ISBN/EAN: 978-94-6259-831-7, Ipskamp Drukkers, 2015
- [17] Aerosonde, [Online]. Available: <http://www.aerosonde.com/>.
- [18] "First atlantic crossing by an Unmanned Aircraft," Barnard Microsystems, [Online]. Available: http://www.barnardmicrosystems.com/UAV/milestones/atlantic_crossing_1.html.
- [19] E. Van Kampen, "*AE4-301 Automatic Flight Control System Design*," Delft University of Technology, Delft, 2015.
- [20] "Dr. One," Drones for development, [Online]. Available: <http://www.dronesfordevelopment.com/>.
- [21] A. Fitzgibbon, M. Pilu and R. B. Fisher, "Direct Least Square Fitting of Ellipses," *Transactions on Pattern Analysis and Machine Intelligence*, vol. 21, no. 5, pp. 476-480, May 1999.

NLR

Anthony Fokkerweg 2

1059 CM Amsterdam, The Netherlands

p) +31 88 511 3113 f) +31 88 511 3210

e) info@nlr.nl i) www.nlr.nl